

amorphous ice, and not semiamorphous ice with a layer structure (7). Yannas (8) predicts a vitrification at $127^\circ \pm 4^\circ\text{K}$ for water, from the depression of vitrification of glycerol by the addition of water. Our measurements are not done at thermodynamic equilibrium and therefore do not exclude such an upper limit for the domain of amorphous ice.

Finally, it is difficult not to mention here the form of liquid water with unusual properties and an unusually high density (1.33 g cm^{-3}) (9), a true polymer of water (10). It does not seem that this polywater, which solidifies at -40°C into a glasslike state, can be directly connected with our observations.

The superdense form of water ice that we have observed at low pressure and low temperature may play an important role in planetary and cometary physics as well as in interstellar grains, as it is likely not to have the same optical or physicochemical properties as ordinary ice, such as refractive index,

albedo, vapor pressure, conductivity, and so forth. However, its importance may be deemphasized in some respects because impurities seem to stop its apparition and its growth.

A. H. DELSEMME
A. WENGER

Ritter Astrophysical Center, University of Toledo, Toledo, Ohio 43606

References and Notes

1. F. Whipple, *Astrophys. J.* **111**, 375 (1950); *ibid.* **113**, 464 (1951); A. H. Delsemme and P. Swings, *Ann. Astrophys.* **15**, 1 (1952); A. H. Delsemme, *13th Coll. Astrophys. Liege* **37**, 77 (1966); B. Donn and G. W. Sears, *Science* **140**, 1208 (1963).
2. P. W. Bridgman, *Proc. Nat. Acad. Sci. U.S.* **47**, 441 (1912).
3. W. B. Kamb, *Acta Cryst.* **17**, 1437 (1964).
4. E. Burton and W. Oliver, *Proc. Roy. Soc. Ser. A* **153**, 1966 (1935).
5. H. König, *Nachr. Akad. Wiss. Göttingen* **1**, 1 (1942); L. Vegard and S. Hillesund, *Avh. Norske Vidensk. Akad.* **8**, 1 (1942).
6. M. Blackman, and N. D. Lisgarten, *Proc. Roy. Soc. Ser. A* **239**, 93 (1957).
7. L. G. Dowell and A. P. Rinfret, *Nature* **188**, 1144 (1960).
8. I. Yannas, *Science* **160**, 298 (1968).
9. B. V. Deryagin and N. V. Churayev, *Priroda* **4**, 16 (1968).
10. E. R. Lippincott, R. R. Stromberg, W. H. Grant, G. L. Cessac, *Science* **164**, 1482 (1969).

2 September 1969; revised 27 October 1969 ■

Mechanochemical Turbine: A New Power Cycle

Abstract. A basic thermodynamic cycle for the production of mechanical power from materials that may be made to contract forcibly and reversibly is described. The cycle differs from existing mechanical power cycles which generally employ expanding fluid as working substances. A "contraction turbine" operating on this cycle has been devised, which has collagen fiber as its working substance and salt solution as fuel and produces mechanical work directly from chemical free energy. Direct conversion of chemical to mechanical energy is routinely effected in muscle but not in usual man-made engines.

The direct conversion of chemical free energy into mechanical motion is routinely effected in muscle but does not occur in usual man-made engines.

In this laboratory mechanochemical engines have been built which do effect the direct conversion (1). We now describe a basic thermodynamic cycle for

effecting direct conversion of chemical to mechanical energy. The cycle provides a general method for the production of mechanical power from any material which may be made to contract forcefully and reversibly. We have devised a new engine operating on this cycle whose features are basic for efficient production of mechanical work from contractile (rather than "expandable") working substances. (In mechanical power cycles expanding fluids are normally used as working substances.)

In the new engine, which we call a "contraction turbine," regenerated collagen fiber (2) cross-linked by formaldehyde is used as working substance, with the reversible contraction that the fiber demonstrates when immersed in concentrated aqueous salt solution, such as LiBr, CaCl_2 , MgCl_2 , and KSCN, producing mechanical shaft work.

Figure 1 shows the variation of force (per unit of dry cross-sectional area) with length of collagen fiber in contact with aqueous solutions of LiBr at various concentrations (3). At zero tension the specific length of this particular collagen fiber in 8M aqueous LiBr solution (L_0) is 60 percent of its specific length in water (L_w). A tension of 52 kg/cm² of cross-sectional area is required to maintain the salt-treated fiber at its salt-free length (L_w). The fiber can be repeatedly moved between states on Fig. 1, by subjecting it to the indicated salt concentration and tension, although some degeneration of fiber properties occurs after 100 or more cycles.

These characteristics of collagen in LiBr (and in similar aqueous salt solutions) are exploited to produce mechanical work continuously by subjecting the collagen to the ideal cyclical

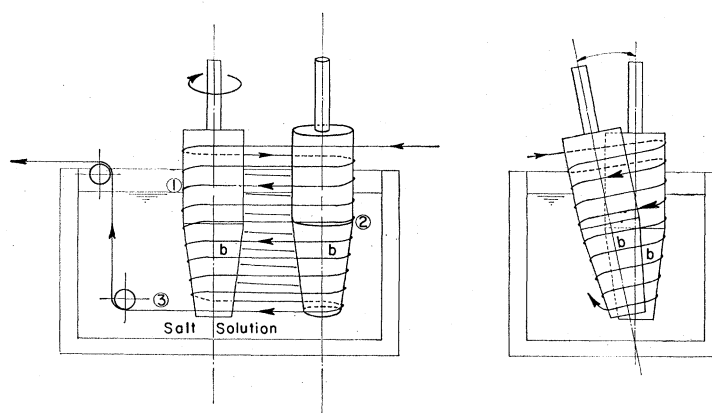
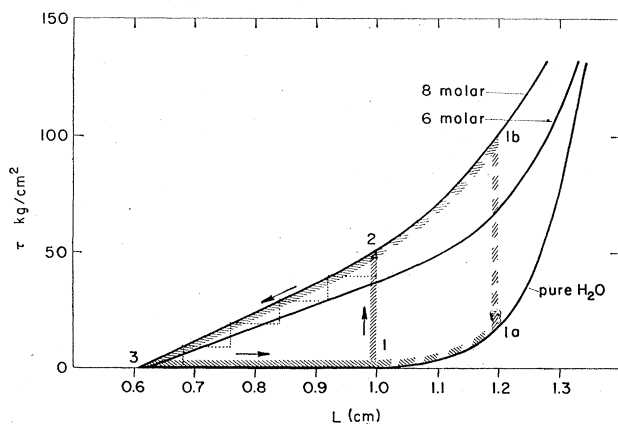


Fig. 1 (left). Tension-length dependence of collagen fiber in LiBr (2). Fig. 2 (right). Contractile fiber-actuated turbine. Front and side views. Fiber tension builds up on cylindrical spindle sections between (1) and (2) at constant specific length. Stepwise contraction occurs between (2) and (3) as the fiber helix descends the conical portions of the spindles (b).

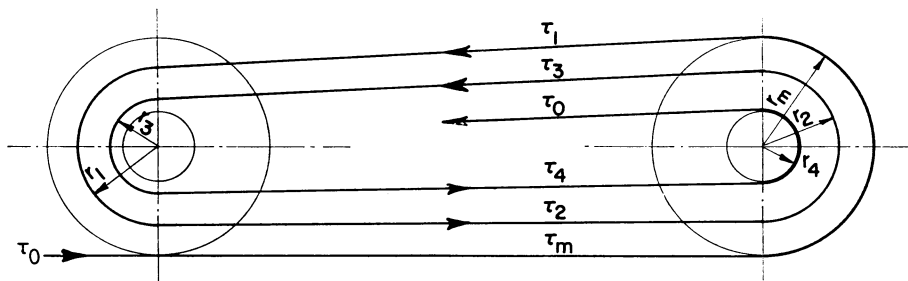


Fig. 3. Contraction turbine. End view showing a four-stage contraction process.

process 1-2-3-1 (hatched marks in Fig. 1). At 1, water-washed collagen fiber, having specific length L_w and substantially zero tension, is constrained so that it cannot shrink, and brought into equilibrium with a concentrated LiBr solution. There it absorbs salt and experiences an isometric tension increase (path 1 to 2). The tensed fiber then releases its elastic energy as work by shrinking reversibly along the $8M$ tension length line (path 2 to 3), from maximum tension (at 2) to near zero tension (at 3). (For shrinkage to occur reversibly, the fiber must act against a force which decreases at the same rate as the fiber tension; or the fiber must contract in many small discrete steps, opposed at each step by a force corresponding to the tension at that step.) The cycle is closed by equilibrating the contracted salt-laden fiber with fresh water, and during this process it loses salt and expands to the initial state (path 3 to 1). The cycle may now be repeated.

A practical cycle based on the above ideal cycle was realized by devising means for isometrically tensioning and reversibly contracting the working fiber in a continuous and repetitive fashion. Isometric tensioning of a moving fiber was achieved by using a pair of canted (slightly tilted axes) cylindrical spindles (Fig. 2). Fiber wrapped about a pair of such spindles spontaneously follows a helical path as the spindles rotate. (The helix pitch depends on the axis angle and the spindle diameter.) The spindles run partially submerged in concentrated LiBr. Washed collagen fiber at a tension and specific length corresponding to state 1 (Fig. 1) contacts the spindles above the LiBr solution. After two full turns about both spindles, the specific length of the fiber is fixed at L_w because (i) both spindles have identical surface speeds and (ii) friction between fiber and spindle prevents fiber slippage. So constrained, the collagen spirals down the spindle surface into the LiBr solution where it absorbs salt

and experiences a sharp tension rise (path 1 to 2, Fig. 1).

A nearly reversible contraction work process is achieved when conical extensions are placed on each tensioning spindle (b ; Fig. 2) which function as a multiple-stage contraction turbine. The contractile fiber, in passing helically

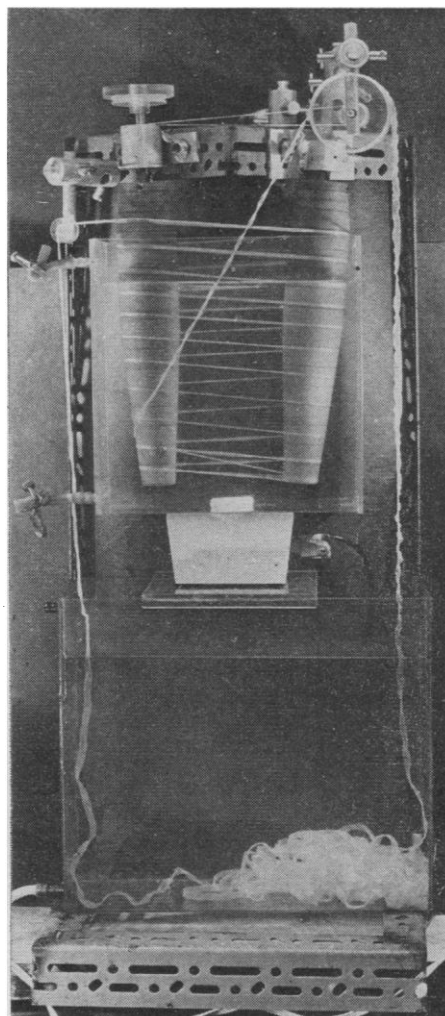


Fig. 4. Contraction turbine actuated by collagen-LiBr. Upper tank contains turbine spindles immersed in LiBr solution. Lower tank is the regenerating (water) bath. Endless collagen fiber loop moves through the cycle in a clockwise direction. Power takeoff is horizontal pulley on upper left.

from one conical spindle to the next, moves repeatedly from a larger to a smaller radius surface, contracting at each pass by a fraction equal to the ratio of the radii. The fiber therefore follows a process resembling the dotted steps in Fig. 1.

The operating principle of the contraction turbine is further illustrated in Fig. 3, which views the turbine's conical spindles from their low tension end, showing the inwardly spiraling path assumed by the working fiber as it contracts. The fiber tension in each stage (or interspindle passage) is a function of the fiber's specific length in that stage as given by the $8M$ line in Fig. 1. Each successive fiber pass between spindles has a lower tension than the preceding pass. In moving from a larger spindle radius to a smaller one, the fiber exerts a net torque at each pass in the direction of motion. The total torque for the configuration in Fig. 3 is

$$T_t = \tau_1(r_m - r_1) + \tau_2(r_1 - r_2) + \tau_3(r_2 - r_3) + \tau_4(r_3 - r_4) \quad (1)$$

Generally for an n stage contraction turbine, total torque T_n , is

$$T_n = - \sum_{i=1}^n \tau_i \Delta r_i \quad (1)$$

where τ_i is the tension in the i stage and Δr_i is the radius decrease in that stage.

If the fiber tension in $8M$ salt is linearly dependent on length between L_w and L_n , then the tension in the i th stage is

$$\tau_i = K(L_i - L_n) \quad (2)$$

where K is a proportionality constant. Equation 2 may also be written

$$\tau_i = KL_w \left(\frac{r_i}{r_m} - C \right) \quad (3)$$

where C is the total contraction ratio, L_n/L_w .

Substituting Eq. 3 into Eq. 1

$$T_n = - \sum_{i=1}^n KL_w \left(\frac{r_i}{r_m} - C \right) \Delta r_i \quad (4)$$

and taking Δr_i to be $[(1 - C)/n]r_m$, Eq. 4 becomes

$$T_n = \frac{n-1}{n} \left(\frac{KL_w r_m}{2} \right) (1 - C)^2 \quad (5)$$

Equation 5 shows that a relatively small number of stages suffice to develop a major part of the maximum possible torque (T_z). For example, for a ten-stage turbine

$$T_w/T_z = 0.9 \quad (6)$$

Since each complete turn of the fiber helix encompasses two contraction

stages, a five-turn helix comes within 90 percent of reversible contraction (T_*).

Operation is made continuous by forming the fiber into a closed loop and disposing the spindles and water bath so that the fiber loop passes from one bath to the other.

The maximum mechanical work that can be obtained from collagen fiber moving through the 1-2-3-1 cycle is the area enclosed by the ideal cycle on the tension-length plane (Fig. 1). For fibers having a specific length (dry) of 270 cm/g and a density of 1.3 g/cm³, this area (maximum or reversible work) is 7.85×10^6 erg per gram of fiber. Consequently a turbine, such as that shown in the Fig. 4 photograph, which has a collagen throughput of 0.09 g/sec, has a maximum or ideal power output of 70 mw. Our actual turbine has delivered about 30 mw, corresponding to a mechanical efficiency of 40 percent.

Free energy conversion efficiency (ratio of work output to free energy of dilution of the salt solutions consumed) is at present considerably smaller (> 1 percent) than the mechanical efficiency, because relatively large quantities of salt solution and wash water cling to the fiber surface and are mechanically carried from one bath into the other, mixing without contributing to the engine output. This deficiency can probably be reduced by incorporating fiber-wiping devices in the cycle.

The work output per cycle can be augmented if the water-washed fiber is slightly elongated (pretensioned) before immersion in salt solution, as shown by the cycle 1-1a-1b-2-3-1 (Fig. 1). Pretensioning is achieved by placing short inverted conical sections immediately above the cylindrical portions of the turbine spindles. Collagen working fiber can also be fueled with CaCl₂, MgCl₂, KSCN, and other aqueous solutions. We have in fact operated the turbine in brine taken directly from the Dead Sea.

The turbine and power cycles described here may be employed with any linearly disposed contractile material which undergoes an appreciable reversible shrinkage or tension increase (or both) when subjected to a change in its environmental potential. The environmental change may be other than chemical. For example, a thermally powered contraction turbine can be operated with linear crystalline polyethylene or rubber working fibers, provided that a heat bath replaces the salt bath and a cooling zone replaces the water regenerating bath.

It is thermodynamically possible to

operate all of these cycles backward as pumps so that the foregoing thermal engine would function as a refrigerator or air conditioner which uses an elastomeric refrigerant.

M. V. SUSSMAN*

A. KATCHALSKY

Polymer Department, Weizmann
Institute of Science, Rehovot, Israel

References and Notes

1. A. Katchalsky, I. Steinberg, A. Oplatka, A. Kam, U.S. Patent No. 3,321,908, 30 May 1967; I. Steinberg, A. Oplatka, A. Katchalsky, *Nature* **210**, 568 (1966).
 2. The collagen fiber, manufactured by Ethicon Corp., Somerville, N.J., is cross-linked by treatment with 0.5 percent formaldehyde before it is used.
 3. M. Levy, unpublished data on the force-length dependence of collagen fiber after repeated contractions and expansions.
 4. Supported by NIH special research fellowship 1F3-GM-36,897-01 (to M.V.S.).
- * On leave from the Department of Chemical Engineering, Tufts University, Medford, Mass.
- 3 June 1969; revised 22 August 1969

Evidence for Solid Carbon Dioxide in the Upper Atmosphere of Mars

Abstract. The infrared spectra recorded by Mariner 6 and 7 show reflections at 4.3 microns, which suggest the presence of solid carbon dioxide in the upper atmosphere of Mars.

In each of the Mariner 6 and 7 missions to Mars (1), the infrared spectrometer (2) recorded spectra in the 4- μ region as the field of view passed through the atmosphere on the bright limb of the planet. This occurred three times and each time a reflection spike was recorded at 2346 ± 10 cm⁻¹, at the center of the ν_3 absorption band of CO₂. No such reflection was observed in either of two dark limb crossings. Figure 1 shows the three bright limb observations. Figure 2 shows again the second Mariner 7 limb crossing in addition to the spectrum recorded 20 seconds earlier (off the limb) and that recorded 10 seconds later (over the planet). Figure 3 shows a laboratory "reflection-absorption" spec-

trum of 15 μ of annealed solid CO₂ (Matheson) condensed at 77°K on a stainless steel plate that filled the field of view of a flight model spectrometer identical to the Mariner instruments (3). With thicknesses exceeding a few microns, a reflection spike is observed due to the index of refraction variation (4) through the 4.3- μ absorption band of CO₂.

It is clear that the reflection spikes displayed in Fig. 1 are highly characteristic and are attributable to solid CO₂. They are surely not due to solid CO₂ on the planetary surface viewed with stray light from outside the principal field of view of the spectrometer. Local surface temperatures at these latitudes exceed 250°K, much too high to permit condensation on the surface. Furthermore, reflection at 2346 cm⁻¹ from the surface would not be observed because the atmosphere is opaque at this frequency. The reflection must be associated with solid CO₂ at such high altitudes that the atmosphere is no longer optically thick.

Trajectory calculations (5) provide geometrical parameters that help to interpret these observations. Table 1 lists the slant range to the point above which the center of the field of view passes closest to the planet, the latitude and longitude of this point, and the aperture width at this slant range. For the second Mariner 7 limb crossing, it is possible to deduce the time between the reflection spike observation and the limb crossing as 5.5 ± 1.5 seconds. This corresponds to an altitude of the optical path at closest approach of 25 ± 7 km.

If it is assumed that this reflection originates over the field of view's closest approach point, the condensation of CO₂ gives an indication of the temperature at this altitude (T_h). The value of T_h so derived, based on an assumed scale height of 8 km, is 130°K.

There are other infrared absorptions that may also be connected with solid CO₂ in the atmosphere—solid CO₂ ab-

Table 1. Conditions under which reflection at 2346 cm⁻¹ was observed by Mariner 6 and 7 in 1969.

	Mariner 6	Mariner 7	Mariner 7
Date	30 July	4 August	4 August
Time	5:19:07	4:43:23	4:54:55
Latitude	2.5°S	22°N	3°S
Longitude	300°E	343°E	355°E
Local time	Noon	Late morning	Noon
Surface temperature		~250°K	~275°K
Slant range	8180 km	9830 km	6500 km
Aperture width	11 km	17 km	11 km